

Rafal Sienicki, Danielle J. Edwards, Manuel A. Cervera, Philip H. W. Leong

Abstract—The process of feature identification in ionogram images and subsequent derivation of ionospheric parameters, known as ionogram scaling, enables the characterisation of the ionospheric propagation conditions of radio waves in the High Frequency (HF) band. Manual ionogram scaling is a time intensive and laborious activity, hence numerous techniques have been developed by many researchers to automate this task.

This article presents a review of the various automatic scaling approaches applicable to vertical, oblique and backscatter ionograms. In addition, we provide a set of recommendations to guide and stimulate further research in this field.

I. INTRODUCTION

The ionosphere is a region of the Earth's atmosphere which contains free electrons and is able to refract HF (3–30 MHz) radio waves. This can be exploited to enable long range, beyond line-of-sight capabilities such as remote sensing, communications and surveillance. The ionosphere is a highly dynamic medium that varies temporally and spatially over many different scales, hence characterisation of the ionosphere is crucial for the effective operation of any HF system.

Ionospheric sounder equipment is used to measure and quantify the properties of the ionosphere by the transmission and reception of HF radio waves. Vertical Incidence Sounders (VIS) and Oblique Incidence Sounders (OIS) are typically used for this purpose. A VIS measures the ionospheric properties directly above (the receiver and transmitter are co-located), whilst an OIS measures the ionosphere at the midpoint between a transmitter and a receiver several hundreds or thousands of kilometres away. VIS, and to a lesser extent, OIS systems are widely deployed around the globe for the purpose of global ionospheric characterisation (Reinisch and Galkin, 2011).

The Backscatter Sounder (BSS) is another type of sounder system. These systems receive the ionospherically propagated

radio waves from the transmitter via backscatter from the ground or sea. Consequently, BSS systems require a greater transmit power and are more complex than VIS and OIS systems. They are useful for the support of a long range surveillance radar, such as Over-the-Horizon Radar (OTHR) due to their similar two-way propagation paths (Earl and Ward, 1987).

The return signal strength when displayed as a function of group range¹ vs. radio wave frequency is known as an ionogram. These ionograms are evaluated to identify critical features and parameters that subsequently can be used to infer the properties of the ionosphere and the ionospheric propagation conditions. This process is called ionogram scaling². Traditionally, ionogram scaling has been performed by ionosphere subject matter experts; however, manual scaling is a time intensive and laborious activity and hence numerous automatic scaling techniques have been investigated and developed over the last few decades. The vast majority of automated scaling algorithms have been applied to VIS ionograms, and to a lesser extent, OIS ionograms, with limited attention to BSS ionograms. Automated scaling tools such as POLAN (Titheridge, 1985), ARTIST (Reinisch and Xueqin, 1983), Autoscala (Scotto, 2001) and DST-IIP (Heitmann and Gardiner-Garden, 2019) have been demonstrated to reliably extract critical features in VIS ionograms. These tools are widely cited and are recognised as authoritative tools in the ionospheric

¹Time-of-flight of the radio wave multiplied by the speed of light in vacuo.

²In this paper, the term ‘scaling’ is used in reference to all ionograms recorded by the three sounder types. The authors acknowledge that the term does not have the same meaning for VIS/OIS and BSS ionogram categories. In the former case, scaling refers to ionogram feature identification and parameterisation of ionospheric properties (Piggott and Rawer, 1978) e.g. critical frequency, minimum virtual height. This is the conventional interpretation of the term in the ionospheric research community. In the latter case, the term refers to a more limited operation. Here, scaling refers to the identification of features from which information regarding the propagation modes may be inferred, without any subsequent ionospheric parameterisation.

research community. OIS are not as widely used as VIS; consequently there is a lack of OIS scaling tools that match the pedigree of aforementioned VIS scaling tools; however, details of several algorithms have been published (Redding, 1996; Hu et al., 2015; Ippolito et al., 2016; Heitmann and Gardiner-Garden, 2019).

The scaling of BSS ionograms is more challenging and the least mature. The integration of returns from multiple propagation modes and antenna sidelobes, the variable ground backscatter, and the reduced number of non-ambiguous, visually discernible image features increases the scaling complexity. Consequently, very few publications exist that detail methods and techniques for automated backscatter ionogram scaling.

This article presents a literature review of the various automatic scaling approaches applicable to vertical, oblique and backscatter ionograms. To the best of our knowledge, this is the first comparative review of scaling approaches across all sounder types. Whilst some VIS scaling investigations (e.g. see Lynn (2018); Heitmann and Gardiner-Garden (2019); Xiao et al. (2020) include a summary of relevant techniques and methods, a dedicated comparative review across all sounder types has not been published.

II. MOTIVATION

Characterisation of the ionosphere is a critical requirement for operation of systems that use the ionosphere to provide a beyond line-of-sight capability such as communication, surveillance or remote sensing. Inference of ionospheric propagation properties at the transmission reflection point is important for frequency management, calibration and performance optimisation of operational HF systems (Earl and Ward, 1987). The structure of the ionosphere is highly non-stationary and varies according to diurnal, seasonal and solar cycle variations, as well as space weather induced phenomena, and hence ionospheric measurements are critical for accurate characterisation of the ionosphere (Earl and Ward, 1987).

An ionogram records the return signal strength of sounder transmission signals propagated via the ionosphere. The return signal strength is typically represented as a two dimensional image, with frequency on the x-axis and group range on the y-axis. Usually VIS ionograms use half the group range, referred to as virtual height³, on the y-axis. Samples of ionogram images pertaining to vertical, oblique and backscatter sounders are shown later in Sections VI and VII. Critical scaling features are labelled in these figures and indicate those features that are ideally identified by an automated scaling algorithm.

Ionogram scaling features are visually discernible as a series of curved, connected trace segments representing a pattern of signal strength variation that is governed by the ionospheric propagation conditions. Each type of sounder produces unique trace segment patterns (features). Visual discernment of the critical features in ionograms is complicated by noise, interference, sounder equipment failures, returns from “unusual”

³The radio waves are retarded by the ionosphere and so the measured, or virtual, height is greater than the true height of reflection.

ionospheric layers (e.g. sporadic E layers, described later) and ionospheric disturbances. The effects of these phenomena can be observed on an ionogram as distortion, smearing, blurring and masking of important ionogram features.

Parameterisation of the ionogram image enables the tuning of electron density model parameters to produce a representative electron density profile based on the collected ionospheric measurements (Cervera et al., 2021). The characterisation of the electron density distribution profile is a highly complex undertaking due to the non-stationarity, inhomogeneity and scattering properties of the ionosphere. However, the electron density vertical profile can be estimated if certain assumptions are applied. The Quasi Parabolic Segments (QPS) model (Dyson and Bennett, 1988; Gardiner-Garden et al., 2018) is one example. In this model, the electron density profile is defined by a set of quasi-parabolic functions that parameterise the main refracting layers of the ionosphere (viz. the E, F1 and F2 layers). The ionogram scaling parameters are used to define the coefficients of the quasi-parabolic functions pertaining to E, F1 and F2 ionospheric layers.

The task of ionogram scaling is recognised as both an art and a science (Hunsucker, 1991). Whilst accurate interpretation of ionogram features requires a deep understanding of the ionospheric physics and HF radio-wave propagation, identification of features, and interpolation and extrapolation of traces often requires a judgement call by an expert. It is therefore not uncommon to obtain variations in outputs even when the scaling is executed by a group of ionospheric Subject Matter Experts (SMEs). This is particularly true for analysis of ionograms captured in disturbed ionospheric conditions. The subjective aspect of ionogram scaling is exacerbated for ionograms recorded by a BSS. Moreover, it is possible for no viable scaling solutions to be available for ionograms recorded during disturbed or anomalous ionospheric conditions and/or contaminated with high level of noise and interference.

III. OVERVIEW AND SCOPE

Research on approaches and techniques for automatic ionogram scaling started in the 1960’s (Wright and Fine, 1960; Doupnik and Schmerling, 1965; Becker, 1967) and numerous toolsets have been developed to perform this function. This article details a comprehensive review of key features, image artefacts and attributes of VIS, OIS and BSS ionograms, and relevant scaling techniques and evaluation metrics.

Section IV introduces the ionogram scaling workflow to provide context for the importance of ionogram feature identification and parameterisation.

Sections V, VI and VII review ionogram features and automated scaling techniques for each sounder type. To the best of our knowledge, this is the first comparative review of scaling approaches across all types of ionospheric sounder systems.

Section VIII reviews the metrics applied for the evaluation of ionogram scaling performance.

Section IX examines the influence of space weather, ionospheric disturbances and sounder failures on ionogram feature characteristics and corresponding scaling challenges.

Over the last decade there has been an increase in the number of publications covering Machine Learning based investigations for application to automatic ionogram scaling. To this end, Section X reviews and compares the merits of ML approaches for this use-case.

Section XI concludes this article with a set of findings and recommendations to guide and stimulate further research in this field.

A brief overview of the physics of the ionosphere, space weather and sounder system design and configuration is included in this article to provide context for ionogram feature interpretation. This material will be beneficial to readers that do not have an ionospheric physics background.

In this review, we focus solely on ionograms recorded by bottomside ionospheric soundings. Topside, transionospheric and reverse transionospheric sounding systems are not considered (Davies, 1990).

IV. IONOGRAM SCALING WORKFLOW

The ultimate goal of ionogram scaling is to provide an estimate of the ionospheric properties and propagation conditions derived from sounder measurements. The ionogram scaling process involves a sequence of steps that are undertaken to enable inference of an electron density distribution model based on an input ionogram. The workflow for an end-to-end ionogram scaling process can be described as:

- 1) pre-processing⁴ an ionogram image to reduce the effects of background noise (denoising) and interference ,
- 2) identification, separation and extraction of dominant traces and features,
- 3) derivation of critical ionospheric parameters from the extracted traces, and
- 4) derivation of the electron density vertical profile, a process referred to as ionogram inversion (Harris et al., 2016).

A visual depiction of the workflow for ionogram scaling and inversion is presented in Figure 1. The focus of this paper is on the feature identification and ionogram parameterisation steps of the ionogram scaling workflow.

V. VERTICAL INCIDENCE SOUNDER (VIS)

The VIS, also known as an ionosonde, is a HF radar that measures the vertical structure of the ionosphere directly above the instrument. The VIS sweeps up in frequency through the HF band and measures the time delay of the returns from the ionosphere. The height that each frequency is reflected from provides information about the different ionospheric layers. Figure 2 shows the configuration of a VIS system for vertical probing of the ionosphere.

⁴Pre-processing is an important pre-requisite step in the scaling workflow. Techniques such as signal processing (e.g. fourier transform (Netherway et al., 2018)), image processing (e.g. morphological operators (Hu et al., 2015), edge detection (Arikan et al., 2002)) and filtering (e.g. size contrast filter (Theera-Umpon, 2007), grayscaling (Fagre et al., 2021), thresholding (Fagre et al., 2021; Song et al., 2016) have been investigated for ionogram preprocessing.

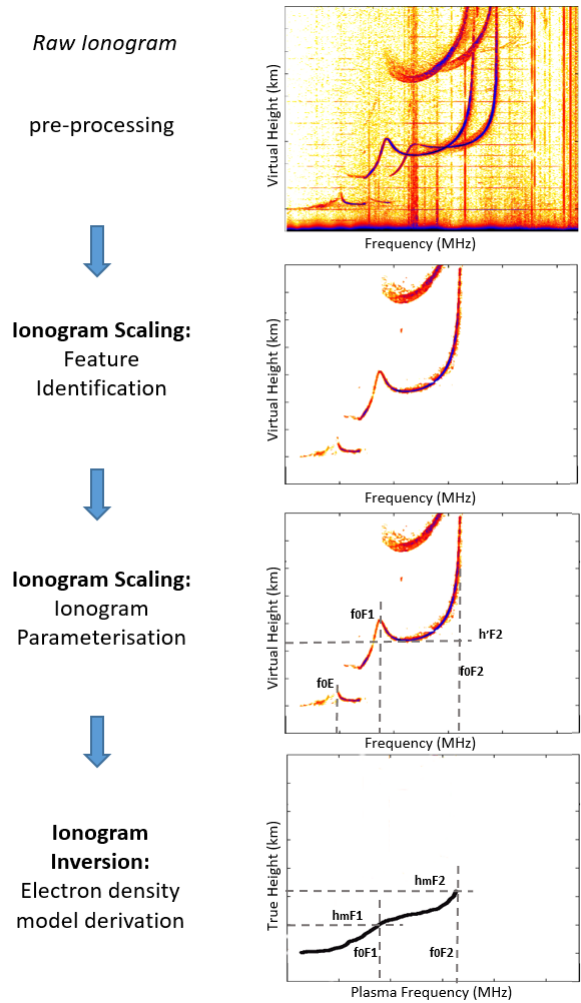


Fig. 1: Workflow for VIS ionogram scaling. A sounder is used to record the return signal strength as a function of frequency. These measurements are formatted into an image known as an ionogram. Analysis of return signal strength intensity variation and shape (profile) of ionogram traces is used to identify key ionogram features that can subsequently be used to derive ionospheric parameters. This process is known as ionogram scaling. These parameters can be used to derive an estimate of the overhead electron density profile. This process is known as ionogram inversion.

Early VIS instruments measured the travel time of the ionospherically propagated radio waves to obtain the virtual height of reflection. With the addition of digital receiver technology, modern instruments such as the Lowell Digisonde (Reinisch and Galkin, 2011) also evaluate the angle of arrival, polarisation and Doppler shift of the reflected signals. This provides additional information to aid in the ionogram scaling.

The VIS is more commonly used than the OIS or BSS as it only requires a single site, operates at a lower power than is required for a BSS, gives a direct measure of the ionospheric critical frequency, and the exact location of the ionosphere that is being probed is more precisely known. Global networks of VIS systems have been established over time with large

long term datasets publically available online. The most widely used network and dataset is provided by the Global Ionosphere Radio Observatory (GIRO) (Reinisch and Galkin, 2011). Some examples of other networks and datasets include those hosted by the Australian Space Weather Forecasting Centre (2022) and the SEALION network operated by the National Institute of Information and Communications Technology (NICT) Japan (Maruyama et al., 2007).

For a historical overview of early VIS development, the interested reader is referred to Gladden et al. (1959).

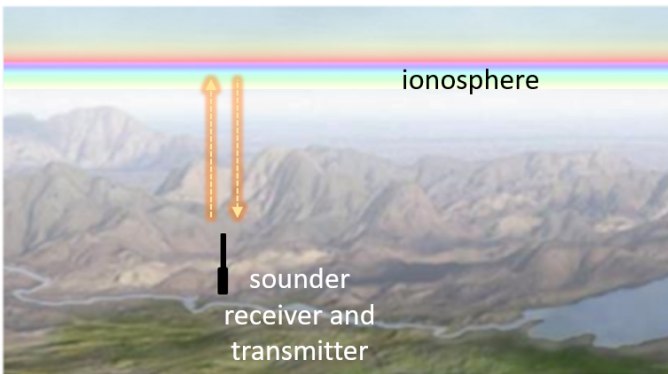


Fig. 2: Simplified diagram (not to scale) showing VIS operation. Sounder signal reflections from the overhead ionosphere can be used to infer the electron density profile.

A. *VIS ionogram features*

A typical VIS ionogram is presented in Figure 3a. The reflection of the sounder transmission signal as a function of frequency and group range is shown as a curved trace with a series of peaks, known as cusps, culminating with the terminal trace segment extending asymptotically to the top of the image (Davies, 1990). The second hop trace (labelled as “2nd hop F2” in Figure 3a) is due to the reflection of the radio waves from the ionosphere to the ground back to the ionosphere then to the receiver. It is not important for deriving ionospheric parameters and will not be discussed further.

Two traces are noted, offset in frequency and group range. This is due to the birefringent⁵ property of the ionosphere causing the radio-wave to split into left and right handed elliptically polarised waves. The trace that asymptotes at the lower frequency is the ordinary (O) mode and the other the extraordinary (X) mode. The O mode is so named as, for vertical propagation, the radio wave is reflected at an altitude where the plasma frequency⁶ of the ionosphere is equal to the radio wave frequency. In the majority of ionograms captured during daytime, it is common to observe up to three cusps, due to reflections from three distinct layers of the ionosphere: the E, F1 and F2 layers. Interpretation of frequency and height

⁵The Earth’s magnetic field causes the refractive index of the ionosphere to have different values depending upon the orientation of the radio wave polarisation.

⁶Plasma frequency f_N is related to electron density N_e by the equation $f_N = (N_e e^2 / \epsilon_0 m)^{1/2}$ (Davies, 1990) where e and m are the charge and mass of an electron respectively and ϵ_0 is permittivity of free space.

parameters of ionogram features corresponding to these layers enables the definition of an electron density profile.

The rapidly increasing retardation of the radio waves with frequency immediately prior to the penetration of the ionosphere results in the corresponding feature being the most visually prominent (left vertical asymptote line labelled in Figure 3a). The frequency at which this feature occurs is known as f_oF2 and is the critical frequency of the ionosphere. Vertically propagating O mode radio waves above this frequency penetrate the ionosphere. The cusps to the left of the f_oF2 feature correspond to the critical frequencies of the E and F1 layers. The frequencies at which these features occur are known as f_oE and f_oF1 respectively.

Virtual height (half of the group range) for the E, F1 and F2 features can be read from the y-axis. Minimum virtual heights corresponding to E, F1 and F2 layers are labelled as $h'E$, $h'F1$ and $h'F2$ respectively in Figure 3a. Note that the virtual height of reflection is greater than the true height due to the retardation of the radio wave.

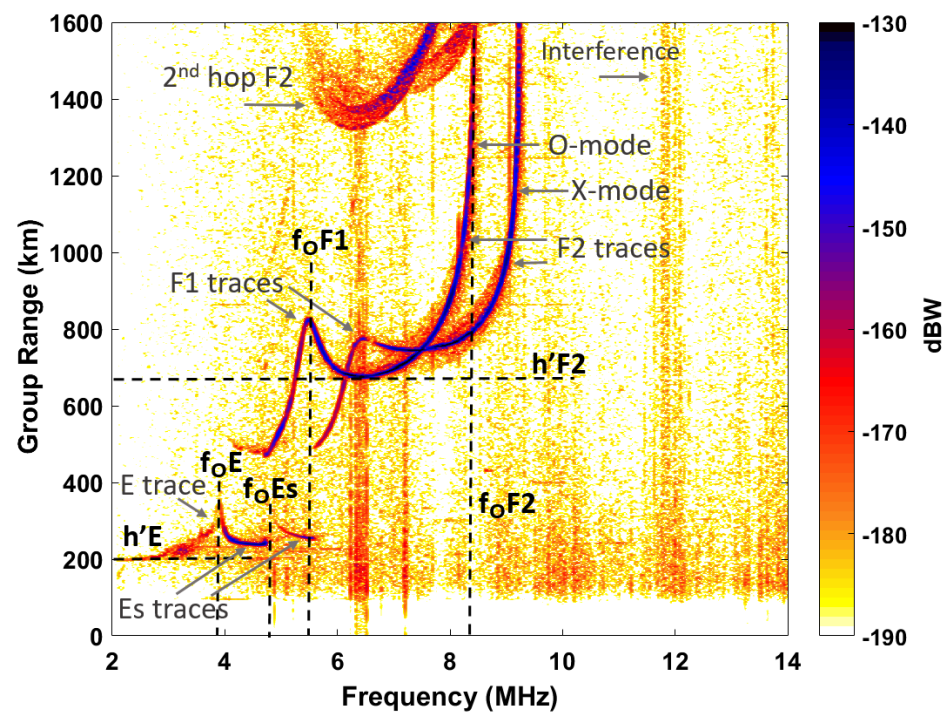
Critical frequency and virtual height parameters for the sporadic E layer, Es, are labelled as f_oEs and $h'Es$ respectively in Figure 3a. The sporadic E layer is a thin layer of metallic ions of meteoric origins that have been concentrated by wind shears in the neutral atmosphere at E layer altitudes (Whitehead, 1989; Haldoupis et al., 2007). In some cases the Es layer can obscure the E and F ionospheric layer returns, especially at lower frequencies (Davies, 1990).

B. *VIS ionogram scaling methods and techniques*

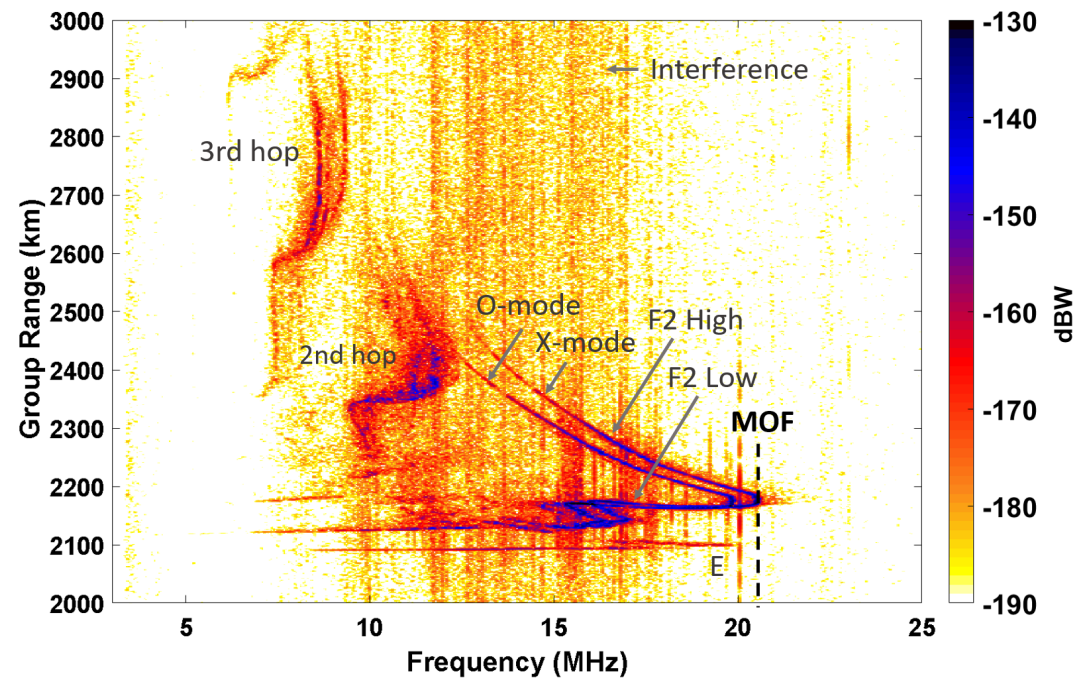
Research into techniques for automated scaling of VIS ionograms started in the 1960’s (Wright, 1959; Doupink and Schmerling, 1965; Becker, 1967) with a large number of publications during the first decade of the 2000s. This era generated a number of scaling software packages, such as POLynomial ANalysis (POLAN) (Titheridge, 1985), Automatic Real Time Ionogram Scaler with True Height (ARTIST) (Reinisch and Xueqin, 1983; Reinisch et al., 2005; Galkin and Reinisch, 2008), Autoscalra (Scotto, 2001; Pezzopane, 2004; Pezzopane and Scotto, 2010) and DST-IIP (Heitmann and Gardiner-Garden, 2019), with ARTIST being the most cited. These packages extract and parameterise the key ionogram features.

The approaches investigated for automatic scaling of VIS ionograms can be loosely categorised into 4 categories: data fitting, template matching, computer vision processing and machine learning. Figure 4 presents a taxonomy of the VIS scaling approaches and techniques, including references.

Data fitting and template matching techniques identify key features by exploiting the ionogram trace curved profile, that typically increases as a function of frequency. **Data fitting** involves iteratively fitting a series of polynomial functions (defined through a set of coefficients) to ionogram pixel data points to find trace segments of interest. Ionogram pixel data points that best align with a base polynomial function are deemed as trace candidates. In a similar manner, **template**



(a) VIS ionogram with key scaling features labelled.



(b) OIS ionogram with key features labelled.

Fig. 3: Sample VIS and OIS ionograms highlighting key ionogram scaling features. Returns from higher order hops and interference artefacts are also labelled.

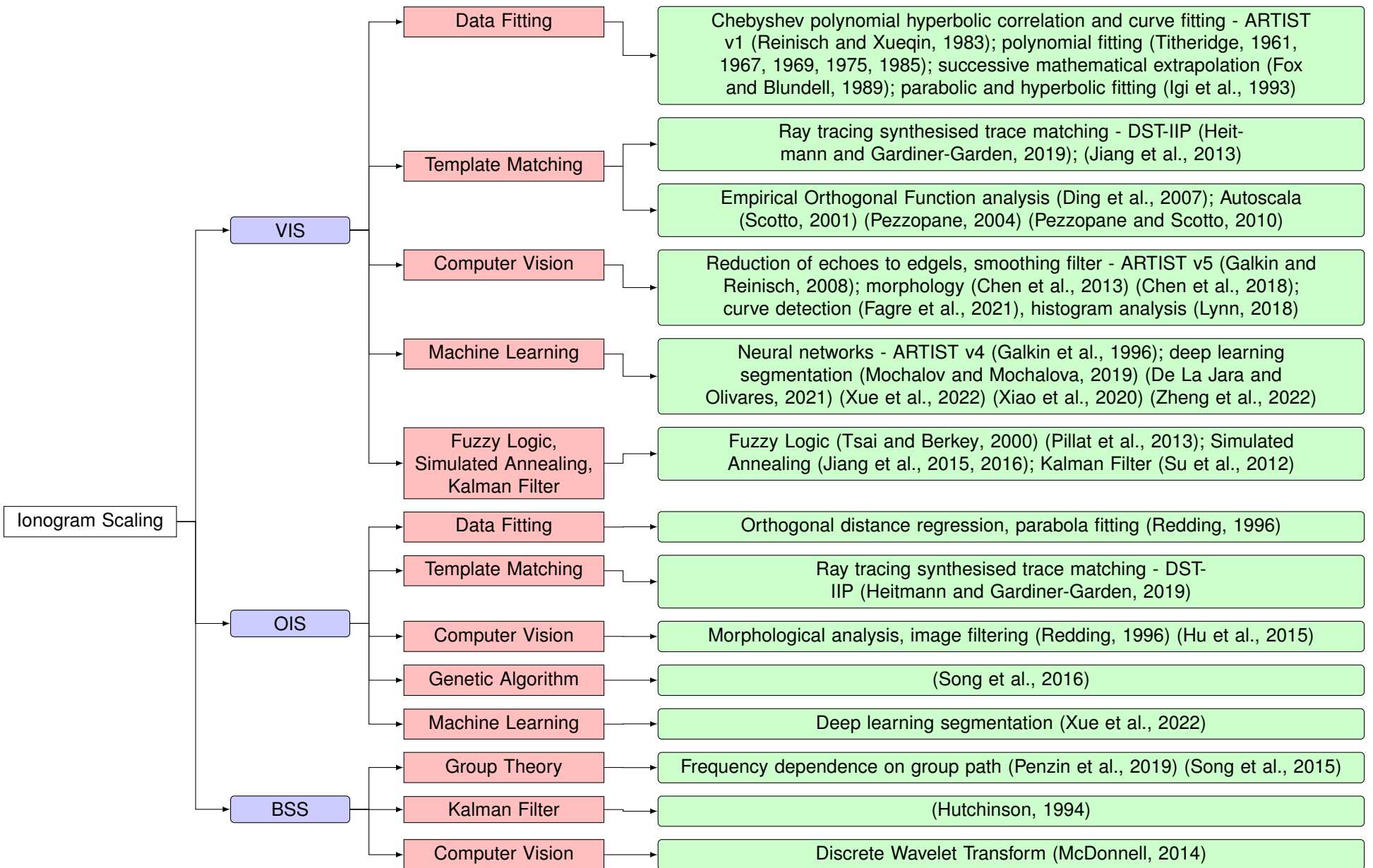


Fig. 4: Taxonomy for scaling techniques for vertical, oblique and backscatter ionograms. References are provided for publications investigated in this review.

	POLAN	ARTIST	AutoScala	DST-IIIP
Era	1980s	1980s + Yes (Global digisonde sounder network)	2000s + Yes (AIS INGV Ionosonde)	2010s + Yes (JORN)
Operational Use	Unknown	1983 1998 (version 4) 2004 (version 4.5) 2008 (version 5)	2001 2004 2010	2019
Year of Publication	1975 1985 1988	Low-Latitude Mid-Latitude High-Latitude	Low-Latitude Mid-Latitude	Mid-Latitude
Latitude Region(s) Applications ⁷	Unknown	Hyperbolic fitting	Image recognition, correlation	Template matching
O/X Polarisation Data Requirement	No	Yes	No	No
Inversion Electron Density Model Representation	Yes Polynomial	Yes Chebyshev polynomial	Yes Parameterised model (12 parameters)	Yes Quasi-Parabolic Segments (10 parameters)
Uncertainty	No	Yes	No	Yes ⁸
Confidence Score	No	Yes	No	No

TABLE I: Comparative summary of popular VIS scaling tools.

matching finds VIS traces through a matching operation, but in this case, the baseline fitting functions are derived from empirical data obtained from observed or synthesised ionogram datasets. **Computer vision** based scaling uses image processing techniques such as edge detection, morphology, filtering etc. to detect, cluster and associate pixels for VIS trace identification. **Machine learning** based methods, treat the ionogram feature identification challenge as a black-box problem. These methods rely on a suitable, large training dataset to enable learning of the ionogram semantics.

In addition to the abovementioned methods, techniques such as fuzzy logic and Kalman filter have also been investigated for scaling of VIS ionograms.

It should be noted that the taxonomy depicted in Figure 4 only lists the different scaling approaches. A review of techniques for ionogram parameterisation is not presented in this figure. In many investigations, heuristics are applied to derive height and frequency parameters of the extracted segments. Furthermore, many, if not all, scaling investigations presented in Figure 4, rely on some form of ionogram pre-processing precursor steps to clean, filter and smooth the ionogram ahead of ionogram scaling.

C. Scaling tool review

A short overview of the most common, and cited VIS scaling toolsets is presented in the following sections.

This review has found that ARTIST is the most authoritative and mature VIS ionogram scaling tool. Its pedigree has been established through validation on large ionogram datasets (tens of thousands) recorded by the GIRO Digisonde network (Galkin and Reinisch, 2008; Themens et al., 2022). Furthermore, ARTIST also includes additional information in the scaling output, namely uncertainty and confidence score,

⁷It is expected that all scaling methods are applicable globally but have been verified only in the listed regions.

⁸Uncertainties reported for the extracted features but not the derived ionospheric parameters

that represents scaling quality and data integrity respectively. These tool features increase user trust and confidence in the automated scaling solution. Moreover, many automated scaling investigations treat the ARTIST scaling output as an evaluation baseline (Pezzopane and Scotto, 2005, 2007; Xiao et al., 2020).

Table I provides a tabular based, side-by-side comparison of the most popular VIS scaling toolsets.

POLAN

The POLAN software program (Titheridge, 1985) is a collection of automated scaling techniques that can be applied to VIS ionograms. The program was publically released as a documented software package in 1985 (Titheridge, 1985)⁹; however, the research into the underlying scaling techniques can be traced back to the prior two decades (Titheridge, 1961, 1967, 1969, 1975).

POLAN provides the flexibility to implement a range of scaling methods. Techniques such as linear lamination¹⁰ and variable degree polynomial fitting (including overlapping polynomial analysis) can be combined with least squares to perform the scaling operation (Titheridge, 1985, 1988).

POLAN has been used to support the validation of the ARTIST scaled inverted electron density profile for challenging ionogram captures (Reinisch et al., 1988; McNamara, 2006).

ARTIST

ARTIST (Reinisch and Xueqin, 1983; Galkin et al., 1996; Reinisch et al., 2005; Galkin and Reinisch, 2008) is the most cited automatic scaling technique in the ionospheric literature. It is the most mature and robust automated scaling technique that is used as an evaluation baseline for many scaling investigations.

⁹see github link (<https://github.com/space-physics/POLAN>, 2017)

¹⁰This technique processes a pair of ionogram frequency-virtual height data points sequentially to derive the electron density vertical profile. This is in contrast to trace fitting techniques, where the entire ionogram trace is processed in a single step.

The ARTIST software has been installed in over 70 global Digisonde sounder stations (Reinisch et al., 2005, 2009; Reinisch and Galkin, 2011). The data¹¹ from these stations are used to drive the the Ionosphere Real Time Assimilative Model (IRTAM) model (Galkin et al., 2012). Exposure to large datasets sourced from a global network of sounders has been critical to the success of ARTIST.

ARTIST identifies key traces and corresponding parameters in VIS ionograms using hyperbolic fitting. It was found that a hyperbolic polynomial profile matches well with ionogram cusp features, including the F2 ionospheric layer asymptotic cusp feature. See Reinisch and Xueqin (1983) for ARTIST scaling algorithm details.

Early versions of the algorithm exhibited some deficiencies, e.g. incorrect F layer critical frequency parameterisation due to gaps in the F layer trace caused by spectrum management restriction or interference (Reinisch et al., 2005), poor performance of scaling of ionograms that exhibited ionospheric disturbances, such as spread F (Galkin and Reinisch, 2008), or reliance on polarisation tag parameters to differentiate between O and X traces. However, the ARTIST software package has evolved into an operational, reliable and robust scaling application. Tool enhancements such as reverse inversion¹², leading edge detection and spread F detection have improved the scaling performance of ARTIST (Galkin and Reinisch, 2008).

Published ARTIST software release versions subsequent to the initial release (Reinisch and Xueqin, 1983) include versions 4.0 (Reinisch et al., 2005), 4.5 (Reinisch et al., 2005) and 5.0 (Galkin and Reinisch, 2008).

ARTIST also includes uncertainty and confidence scores as part of the scaling output. This information is useful for inference of the quality of the scaling product.

An uncertainty band (95% probability) derived from a statistical analysis of historical data referenced for the sounder station of interest, overlaid on the inverted electron density profile derived from the scaled parameters gives insight to the operator on how potential scaling errors translate to ionogram inversion output (Galkin and Reinisch, 2008).

A confidence score quantifies the quality of the input ionogram in terms of data integrity and detected disturbed ionospheric conditions. This score is useful to infer the reliability of the scaling product. See Conkright and McNamara (1997), Galkin et al. (2013) and Themens et al. (2022) respectively, for more information on the confidence score and results from a study conducted to determine its usefulness.

DST-IIP

The DST Ionogram Image Processing (IIP) scaling tool (Heitmann and Gardiner-Garden, 2019) is used operationally to support the generation of the Real-Time Ionospheric Model

¹¹ARTIST is deployed as a software application that produces an XML file output that records the scaling parameters and derived electron density profile.

¹²This term describes the practise of using a representative electron density profile to produce an ionogram trace. The reconstructed trace can subsequently be used to assess the validity of the scaled trace and assist with extrapolation of challenging trace segments.

(RTIM) of the Jindalee Operational Radar Network (JORN) in Australia. This tool has been used experimentally since 2006, operationally since 2011, and has been extensively tested on mid-latitude ionograms from the Australian region.

The DST-IIP algorithm uses a template matching technique for automatic scaling of both VIS and OIS ionograms. The VIS and OIS scaling algorithms are identical; the VIS is treated as a special case of the OIS where the transmitter and receiver are collocated.

The algorithm was designed to be flexible regarding the input ionogram, and so can work on ionograms with variable input image quality, thresholded or non-thresholded ionograms, with and without polarisation information, and does not require angle of arrival or Doppler information, which is not always available.

The DST-IIP constructs a three layer electron density profile (E, F1, and F2), defined by 10 parameters used by the JORN RTIM. The quality and uncertainty of the results are reported, based on the width of the image features and the similarity of the reproduced ionogram trace created using analytical raytracing through the constructed electron density profile.

First, image pre-processing is performed. This procedure estimates the background noise, applies image cleaning, thresholding and oblique range transformation algorithms, and then does basic quality checks on the resultant pre-processed image. The oblique range transformation converts the VIS ionogram to an equivalent oblique ionogram where the transmitter and receiver are separated by 500 km. The scaling algorithm then works its way up the traces from the lower ionospheric layers through to the upper layers, making use of the lower layer information as it moves up through the ionosphere. The initial layer parameters are estimated from empirical climatological models. Image processing and fitting are used to extract the E layer parameters to get the layer height. The F1 layer parameters are based on the climatology. Sporadic-E layer features are extracted directly from the ionogram. F2 layer features are extracted using image processing and an iterative fitting process is applied to find the electron density profile that best reconstructs the observed ionogram trace. For further details on this scaling technique consult Heitmann and Gardiner-Garden (2019).

Autoscala

Autoscala was developed in the early 2000's with the first version being limited to solely scaling the F2 layer feature. A series of improvements were implemented in the same decade to add functionality to scale the F1 (Pezzopane and Scotto, 2008) and sporadic E (Scotto and Pezzopane, 2007) layer features, and be robust to ionograms that record weak (faint) traces (Pezzopane and Scotto, 2010).

Autoscala uses correlation and image recognition techniques (e.g. maximum contrast) (Pezzopane, 2004) to perform automated scaling of VIS ionograms. A suite of representative ionospheric layer traces are iteratively overlaid on an ionogram, and traces that receive the highest correlation score are used to derive the scaling parameters (Scotto, 2001). The fitting procedure uses a pair of traces to detect and scale O and X traces simultaneously. This feature allows the software

to scale ionograms recorded by sounders that do not tag traces with polarisation information (Pezzopane et al., 2010).

VI. OBLIQUE INCIDENCE SOUNDER (OIS)

The OIS is a HF system that measures the structure of the ionosphere between the transmitter and receiver, which are often separated by 500 to 3000 kilometres. An OIS operates similarly to a VIS; it sweeps up in frequency through the HF band and measures the signal strength of the ionospherically propagated radio waves. However, the OIS probes the ionosphere at the mid-point between a transmitter and receiver, while the VIS measures the ionosphere directly above. Figure 5 shows the typical configuration of an OIS system and the oblique propagation path.

An advantage of using an OIS is that it allows for the characterisation of the ionosphere at locations where a VIS cannot be installed, such as over bodies of water. In addition, a network of OIS transmit and receive sites¹³ allows for the probing of the ionosphere at many more locations than a network of the same number of VIS sites, due to the number of combinations of midpoints that can be achieved (Ayliffe et al., 2019). Furthermore, the one-way propagation mode feature makes it an attractive ionosphere characterisation resource for systems that operate in similar propagation modes, such as HF point-to-point communication systems.

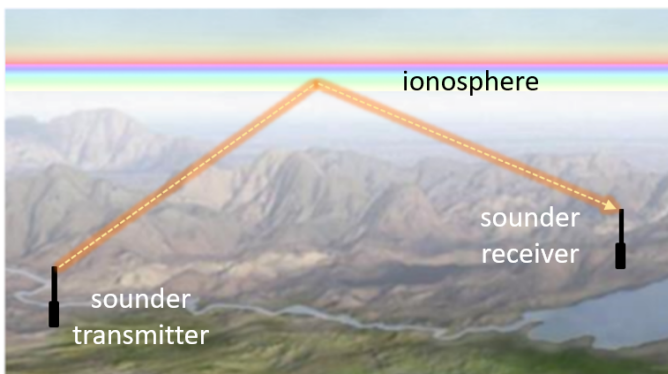


Fig. 5: Simplified diagram (not to scale) showing OIS operation. Signal reflections from the ionosphere can be used to infer the electron density profile at the mid-point between the transmitter and receiver.

A. OIS ionogram features

A sample OIS ionogram is presented in Figure 3b. Similar to the VIS ionogram, the x and y axes of the OIS ionogram are respectively frequency and group range. Due to the increase in maximum frequency that the ionosphere can support as a function of the off-zenith angle of the signal (Davies, 1990), OIS ionogram traces have a larger frequency extent than VIS.

Each layer of the ionosphere is able to support two one-hop propagation paths (at different elevation angles) between the spatially separated receiver and transmitter. This means that if it is able to support propagation, each layer of the ionosphere

will produce a trace at two group ranges, with the shorter due to the low elevation path. The two propagation paths attributed to low and high elevation angles are labelled as low and high rays respectively in Figure 3b. At the ‘nose’ feature of the ionogram, the ray paths corresponding to the high and low rays merge and focusing occurs. This visually distinct feature is a critical OIS scaling parameter known as the Maximum Observable Frequency (MOF).

The MOF is the most common, and, in many automatic OIS scaling algorithms, the sole feature that is scaled. In addition to being an important parameter for inversion, the MOF feature is useful for frequency management support of HF point-to-point systems.

Similar to the issues that arise when scaling parameters from VIS ionograms in the presence of ionospheric disturbances, scaling the OIS MOF is likewise difficult and potentially prone to error. For example, the presence of a sporadic E layer can render the MOF for the E layer to exceed the MOF for the F layer.

Range-transform techniques may be used to convert the OIS ionogram into an equivalent mid-point VIS ionogram to enable simple determination of the parameters describing the ionosphere at the mid-point of the oblique path using VIS scaling algorithms. Each pixel of an OIS ionogram (group range, frequency coordinates) corresponds to a specific pixel on the equivalent VIS ionogram (virtual height, frequency coordinates) (Davies, 1990). This is visually presented in Figure 6. While this technique is often useful and enables ionospheric parameters to be obtained at a location when a VIS cannot be installed, it does make certain assumptions about the ionosphere (spherically symmetric) which introduces errors to the obtained parameters.

B. OIS ionogram scaling methods and techniques

Traditionally, OIS have been used less often than VIS to characterise the ionosphere and consequently research and scaling tool development is less mature. Our review has found that there are fewer publications covering research of scaling techniques for the OIS ionogram in comparison to the VIS ionogram case. The DST-IIP is the most mature OIS scaling tool. A taxonomy of the scaling methodologies presented in Figure 4 summarises the various OIS scaling algorithms. Trace fitting and image processing are the main techniques.

The DST-IIP scaling software described in Section V for scaling VIS ionograms, is also used for the automatic scaling of OIS ionograms. This template matching technique assumes a spherically symmetric ionosphere. A single electron density profile for the mid-point is produced as the final output of the scaling. The F2 layer parameters are fitted using iterative process of analytical ray tracing (ART) and matching the synthetic traces to the observed traces.

VII. BACKSCATTER SOUNDER (BSS)

The BSS, also known as a Wide Sweep Backscatter Ionogram (WSBI) sounder, is a quasi mono-static radar system.

¹³Modern digital receivers can receive multiple OIS transmissions.

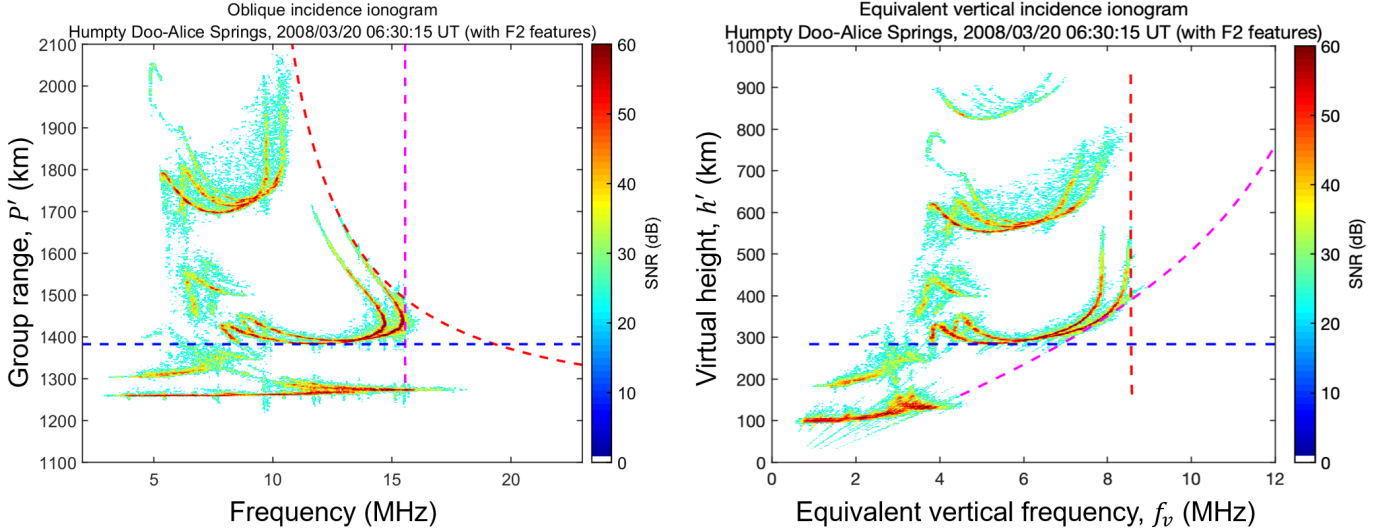


Fig. 6: Range transformation applied to an OIS ionogram (left) to obtain an equivalent VIS ionogram (right) that can subsequently be used to scale critical frequency (red dashed line) and virtual height (blue dashed line) parameters.

The transmitter and receiver are separated by a few tens of kilometers for inter-site isolation purposes, this being negligible considering the long range sky-wave propagation distances involved (thousands of kilometres).

The BSS operates similarly to an OTHR. The transmitted signal propagates via the ionosphere to a distant ground location. Most of the energy of the signal is forward scattered; however, a small amount is backscattered and propagates via the ionosphere to the receiver. Figure 7 shows the typical configuration of a BSS and the backscattered propagation path. The BSS provides ionospheric information over a much larger area than the VIS and OIS. Typically, the transmit antenna has a large beam width (90 deg) and so “floodlights” a large area. Reception is on a linear array of antennas which enables narrow beams to be formed within the transmit coverage. Backscatter ionograms are produced in each of the receiver beams. The BSS requires a much larger transmit power than a VIS or OIS due to the additional losses incurred from the ground scatter and the extra absorption experienced during the double path through the ionosphere. The BSS power requirement is generally of the order of 1-10s of kilowatts, compared to 10s of watts for the VIS and OIS. Similarly to the VIS and OIS, the BSS sweeps up through frequency in the HF band.

The BSS is an attractive sounder resource for the HF OTHR use-case due to the similarities in the propagation paths between the BSS and OTHR. Additionally, physical, practical and legal constraints on VIS and OIS sounder transmitter and receiver placement may render the sounder measurement footprints to have limited overlap with OTHR coverage requirements. In these situations, a BSS is more suitable. BSS measurements may support OTHR real-time ionospheric characterisation, radar frequency management and coordinate registration¹⁴ functions (Earl and Ward, 1987).

BSS systems are not as widely used as the VIS and OIS due to the additional complexity and cost. The design of each system varies depending on the use-case e.g. the use of a quasi-monostatic system with a continuous waveform, or a collocated transmit and receive system using a pulsed waveform, must be considered. The quality of the BSS ionogram scales with the transmit power and range-azimuth resolution. Higher power increases the signal-to-noise ratio, which reveals more ionospheric features within the ionograms. This can reveal complications such as contributions from the receive array sidelobes, which may be problematic for automated scaling algorithms.

Some examples of BSS used operationally to support OTHR are the JORN BSS in Australia (Earl and Ward, 1987; Netherway et al., 2018), and the relocatable over-the-horizon radar (ROTHR) WSBI in the United States of America (Nickisch et al., 2016). The JORN BSS operates over the frequency range 5 to 45 MHz. Two sets of antenna arrays are used to support this; the low (<30 MHz) and high (>30 MHz) band arrays. Transmission is from a vertically polarised log-periodic dipole antenna. Reception is on an array of doublet monopoles, which are able to form beams with appropriate phasing between the receive array elements. The low band transmit system has a transmit power of 10-15 kW, and the high band has a transmit power of 1 kW (Earl and Ward, 1987).

The Super Dual Auroral Radar Network (SuperDARN) radars have the ability to operate as a BSS when not operating in its standard data collection mode (Dyson et al., 2000). Unlike the JORN BSS and ROTHR WSBI, the SuperDARN transmitter and receivers are collocated, and so these radars are pulsed systems. SuperDARN is primarily used for investigating the high latitude ionosphere by measuring the characteristic returns from ionospheric irregularities. However, ionospheric parameters such as the MOF and f_0F2 can be extracted from the radar ground scatter returns (Bland et al., 2014).

¹⁴The conversion of the radar group range to a ground location.

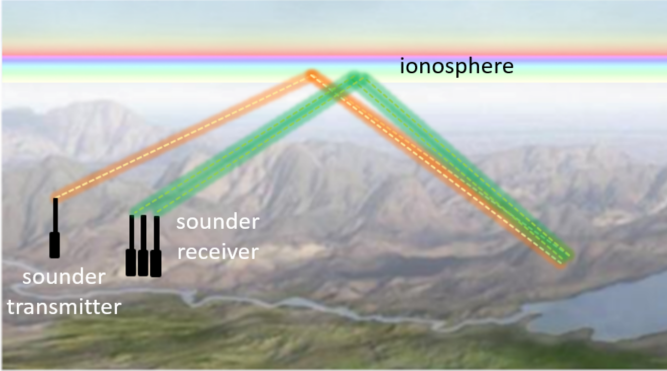


Fig. 7: Simplified diagram (not to scale) showing BSS operation. Ionospherically propagated radio waves from the transmitter (orange dashed line) are scattered by the ground. The ground back scattered signal propagates to the receiver via the ionosphere (green dashed line).

Some low power BSS systems have also been developed, such as the Wuhan Ionospheric Oblique Backscattering Sounding System (WIOBSS) (Chen et al., 2009) and the chirp ionosonde developed by the Institute of Solar-Terrestrial Physics, Siberian Branch of the Russian Academy of Science (Penzin et al., 2019). These pulsed systems have peak transmit powers of 500 W and 1 kW respectively.

A. BSS ionogram features

BSS ionograms display the return signal strength from ground and sea backscatter as a function of sounder transmission frequency and group range. A sample BSS ionogram is presented in Figure 8a. The Leading Edge (LE) is a key feature of a BSS ionogram. A LE is a thin ledge-like feature that is visually discernible as a series of connected, steep signal strength changes. It is the minimum time delay (group range) for the receipt of the backscattered, ionospherically propagated signal as a function of frequency. Multiple LE traces corresponding to propagation via different propagation modes are commonly observed on a BSS ionogram. See Figure 8a for samples of key LE traces. The F2 LE may be interpreted as the “nose” or F2 MOF of oblique ionograms formed from receivers positioned on the ground at successive ranges in the direction of the BSS beam.

Typically, the LE trace exhibits a smooth, low-order polynomial-like profile with the contour line trending upwards in group range as a function of frequency.

Identification and extraction of LE features in a BSS ionogram is a challenging undertaking. Firstly, the LE is a ledge-like feature with undefined start or end points. It does not resemble visually discernible features such as cusps, asymptotic lines or vertices that are present in VIS and OIS ionograms. Secondly, the effects of ionospheric dynamics and sounder characteristics can profoundly influence the LE feature. Consequently, the LE may exhibit intensity variation that can render some aspects of the trace line to be faint, disconnected, or exhibit localised strong curvature features or “kinks”. Thirdly, discrimination logic is required to separate

the LE traces based on refractions from different ionospheric layers (including higher order hops) and magnetoionic splitting. This is complicated by LE traces associated with antenna sidelobe returns (Croft, 1972). See Figure 8b for samples of BSS ionograms that depict the diversity of LE features.

Tables II and III respectively summarise BSS LE feature characteristics and review the influence of sounder configuration on LE feature composition.

B. BSS ionogram scaling methods and techniques

The BSS is significantly more complex and expensive than VIS and OIS, consequently they are not as common. In most use-cases, a BSS is dedicated for support to OTHR operation in a specific region, and not treated as an ionospheric sounder resource for contribution to global ionospheric modelling. Not surprisingly, there are no publicly available BSS datasets. Limited access to BSS system and measurement data has contributed to significantly reduced amounts of research and investigations on automatic scaling of BSS ionograms when compared to VIS and OIS ionograms. This review has found only a few papers that address BSS ionogram LE feature scaling¹⁵. Figure 4 presents taxonomy of the approaches for BSS ionogram LE scaling. Application of the Kalman filter and minimum group path theory are the two main approaches used to perform the LE feature extraction. See Figure 4 for references.

VIII. IONOGram SCALING METRICS

Scaling investigations report performance predominantly using a distance-based metric. A scaling error, defined in frequency and group range dimensions relative to manually scaled parameters, is used to define the scaling accuracy.

Many VIS and OIS¹⁶ scaling investigations reference the URSI handbook of ionogram scaling (Piggott and Rawer, 1978) for reporting and comparing scaling results. This handbook is recognised as an authoritative standard for the evaluation of VIS scaling performance. The handbook defines the resolution of the scaling error. It is specified in terms of the readability of ionogram features for each ionospheric layer. This parameter defines the error margin for recognition of accurate and acceptable scaling performance. This readability parameter is referred to as (Δ) and its values are set as follows:

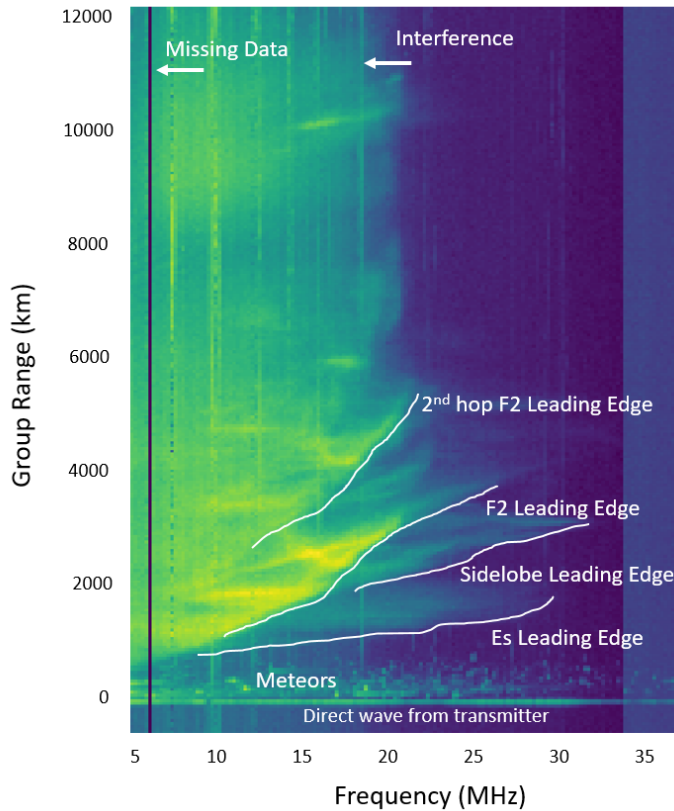
- E layer accuracy (Δ): $\pm 0.05\text{MHz}$, $\pm 2\text{km}$
- F layer accuracy (Δ): $\pm 0.1\text{MHz}$, $\pm 5\text{ km}$

In this handbook, a maximum error of (5Δ) or 20% relative error (whichever is greater) is deemed as acceptable¹⁷.

¹⁵It is possible that more publications on this topic exist, however this review has only considered publications written in English.

¹⁶A dedicated scaling standard for the evaluation of OIS scaling does not exist; however, many investigations adopt the VIS scaling standard (Piggott and Rawer, 1978) for scaling performance evaluation. This practise is deemed acceptable due to the similarity of the features for both ionogram types. The MOF nose vertex of the OIS ionogram is characterised as a distinct feature that can be defined in pixel coordinates, in a similar manner to the cusp features of the VIS ionogram.

¹⁷The URSI handbook treats these scaling results as doubtful. These scaling results are marked with a qualifying letter to indicate a high level of scaling uncertainty



(a) Sample backscatter ionogram with key leading edge features labelled. Meteoric returns and interference artefacts are also labelled. The F2 LE is of primary interest for the OTHR use case.

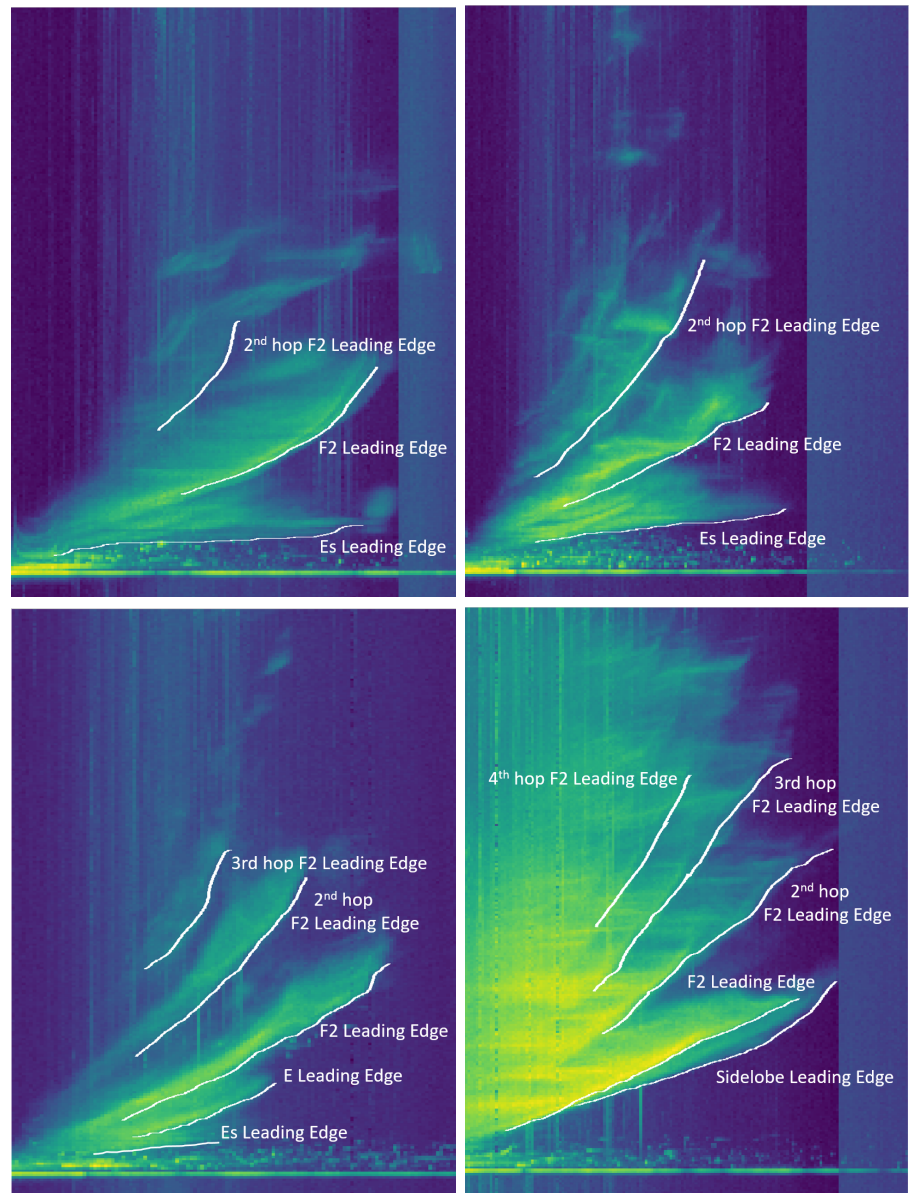


Fig. 8: Backscatter sounder ionogram samples.

BSS Ionogram Scaling Features	Definition and Comments
F2 Leading Edge (F2 LE)	The F2 LE feature represents the minimum time delay (group range) for the receipt of a backscatter signal refracted from the F2 ionospheric layer. This feature is labelled in Figure 8a. The long-range propagation and diurnal stability characteristics of the F2 ionosphere layer makes the F2 LE BSS ionogram feature of primary interest for the OTHR use-case. Multiple F2 LE traces corresponding to higher order hops may be observed on some BSS ionograms. The primary (first hop) F2 LE feature is the most visually prominent trace. In many cases, it may be the sole LE feature that can be identified non-ambiguously.
F1 Leading Edge (F1 LE)	The F1 LE feature represents the minimum time delay (group range) for the receipt of a backscatter signal refracted from the F1 ionospheric layer. The F1 LE is usually masked ¹⁸ by the strong F2 layer and as the F1 layer is absent during nighttime conditions, the F1 LE is not typically observed. For example, this feature is not visible in Figure 8a.
E Leading Edge (E LE)	The E LE feature represents the minimum time delay (group range) for the receipt of a backscatter signal refracted from the E ionospheric layer. Similar to the F1 LE feature, the E layer LE is typically masked ¹⁸ by the strong F2 layer and is usually not observed. This feature is not visually discernible in Figure 8a, but is present in the lower left panel of Figure 8b.
Es Leading Edge (Es LE)	The Es LE feature represents the minimum time delay (group range) for the receipt of a backscatter signal refracted from a Sporadic E (Es) layer. This trace is easily identifiable in ionograms due to its unique characteristics in comparison to the E and F traces. The Es trace is visually discernible in ionograms as a relatively flat line, that is positioned at low group-range values and spans a wide frequency bandwidth. The Es trace feature is labelled in Figure 8a.

TABLE II: Description of the leading edge features of a BSS ionogram.

BSS System Characteristics	Comments
Transmitter power, signal processing	Signal-to-Noise Ratio (SNR) plays a critical role in the definition of the LE feature. Sounder transmit power levels, pulse compression and integration signal processing techniques influence the SNR of the return signal. In general, higher SNR produces more distinct BSS ionogram LE features.
Receive Antenna pattern (mainlobe)	A narrow receive beamwidth antenna configuration generates higher resolution ionograms azimuthally. Consequently, the ionograms are sharper with more distinct LE features which are easier to visually identify and interpret. Conversely, a wide beamwidth antenna configuration generates BSS ionogram LE artefacts that are less sharp due to the integration of propagation returns from a larger spatial footprint. For example, the separate LE features corresponding to O and X propagation mode returns are not easily discernible on an ionogram recorded by a BSS configured with a wide receive antenna beamwidth.
Receive Antenna pattern (sidelobe)	Backscatter signal returns in the receive antenna sidelobes may produce additional LE features as shown in Figure 8a. While the LE features due to sidelobes have lower intensity, they still need to be identified and filtered as part of the scaling process. Additionally, large gradients in the ionosphere during dawn/dusk periods lead to large azimuthal differences in the ionosphere. Thus a sidelobe return from a direction where the ionosphere is stronger may be falsely identified as the F2 LE if the ionosphere in the direction of the main lobe is significantly weaker.
Multiple beams	BSS systems typically are able to form multiple beams azimuthally. It is expected that there exists a spatial relationship across the beams that can be leveraged to interpret LE features across sequential beams e.g. backscatter returns detected in a sidelobe in one beam will be detected in the mainlobe of a different beam.

TABLE III: Influence of BSS sounder operational and design characteristics on leading edge features of a BSS ionogram.

Many scaling investigations report scaling performance results specified in terms of both (Δ) and (5Δ). The former is useful for the inference of absolute scaling performance, whilst the latter is useful for gauging the reliability of ionogram scaling performance i.e. evaluation of the ratio of ionogram scaling results that fall within the maximum scaling error allowed.

Some VIS scaling investigations do not reference the URSI handbook, and instead report performance using histogram or percentile distribution plots. Whilst this is useful for the analysis of scaling error performance, this format makes it difficult to compare results across investigations.

In contrast to the VIS and OIS case, no standard exists for the evaluation of BSS ionogram scaling. Unlike VIS and OIS, the BSS ionogram exhibits an undefined number of reference features (leading edge coordinates), and hence a dedicated evaluation standard is required.

¹⁸The higher level of ionisation in the F2 ionospheric layer relative to the lower E and F1 ionospheric layers has the effect of the F2 returns on a BSS ionogram obscuring the E and F1 LE features.

Table IV provides a summary overview of the ionogram scaling metrics. Note: The metrics presented in Table IV for the BSS ionogram case, represents proposed metrics for consideration based on (Crouch, 2018; Song et al., 2015), but is not recognised an authoritative. See Recommendation 2 in Section XI for further discussion.

IX. EFFECTS OF SPACE WEATHER ON IONOGram FEATURE CHARACTERISTICS

Visual discernment of the critical features in ionograms is complicated by ionospheric irregularities and disturbances, Radio Frequency Interference (RFI) and sounder failures. The effects of these phenomena can be observed on an ionogram as distortion, smearing, blurring or masking of important ionogram features. This increases the complexity of the ionogram scaling process and can lead to ambiguous or mis-classification of ionogram features.

In these situations, a trained human (SME) is required to make sound judgement, and interpolation and/or extrapolation

	VIS	OIS	BSS
Feature	E: $h'E, foE$ F1: $h'F1, foF1$ F2: $h'F2, foF2$	MOF	multiple leading edge points measured in frequency or group range dimension, referenced to a sample surveillance region. Applies to all ionospheric layers.
Baseline	Manually scaled features ¹⁹		
Absolute error (individual ionogram)	Scaling error wrt frequency and group range		Scaling error wrt frequency or group range Evaluated at each leading edge point
Minimum Accuracy (individual ionogram)	E layer $\pm 0.05\text{MHz}, \pm 2\text{km}$; F layer: $\pm 0.1\text{MHz}, \pm 5 \text{ km}$ (based on URSI handbook)		E layer $\pm xx\text{MHz}$ or $\pm xx\text{km}$; F layer: $\pm xx\text{MHz}$ or $\pm xx \text{ km}$ Evaluated at each leading edge point
Acceptable Accuracy (individual ionogram)	E layer $\pm 0.25\text{MHz}, \pm 10\text{km}$; F layer: $\pm 0.5\text{MHz}, \pm 25 \text{ km}$ (based on URSI handbook)		E layer $\pm xx\text{MHz}$ or $\pm xx\text{km}$; F layer: $\pm xx\text{MHz}$ or $\pm xx \text{ km}$ Evaluated at each leading edge point
Scaling Performance Reporting - Accuracy (whole dataset)	Ratio (percentage) of ionograms that satisfy minimum/acceptable accuracy. Reported for each feature.		Ratio of estimated leading edge data points that satisfy minimum/acceptable accuracy. Report for each ionospheric layer.
Scaling Performance Reporting - Recall (whole dataset)	Ratio (percentage) of ionograms for which no features are estimated. Report for each feature.		Ratio of leading edge data points for which no estimates are generated. Report for each ionospheric layer.

TABLE IV: Summary of metrics used for performance evaluation of VIS, OIS and BSS ionograms. Note: No authoritative metrics exist for BSS ionogram evaluation. BSS metrics, displayed as orange cells, are the proposed metrics for consideration.

is often required to complete the feature interpretation process. Tables V and VI provides a summary of the ionospheric disturbances and interference effects and how they effect ionogram feature characteristics.

X. REVIEW OF DEEP LEARNING IONOGram SCALING INVESTIGATIONS

There is a growing interest in the application of machine learning to ionogram scaling. The majority of current investigations have been predominantly applied to VIS ionograms (De La Jara and Olivares, 2021; Xiao et al., 2020; Xue et al., 2022). Machine learning, specifically deep learning convolutional and transformer methods, offer a powerful feature extraction capability (LeCun et al., 2015) that can be leveraged for automated ionogram scaling.

Mochalov and Mochalova (2019) is the first investigation that applies a convolutional U-Net model for the extraction of traces pertaining to E, F1 and F2 ionospheric layer reflections in a VIS ionogram. The investigation by De La Jara and Olivares (2021) improves on the results of Mochalov and Mochalova (2019) by fine-tuning a convolutional encoder-decoder model pre-trained on trace features derived using filtering, clustering and mean shift techniques. Investigation by Xiao et al. (2020) experiments with different convolutional backbones in the Feature Pyramid Network architecture. This investigation achieves a high performance with reported precision and recall of 98% and 90% respectively.

Importantly, in addition to reporting scaling performance using computer vision metrics, results presented by (Xiao et al., 2020) are also conveyed in ionogram domain metrics:

¹⁹This can also be scaling results obtained from an alternate scaling tool if comparison is performed across toolsets.

frequency and group range error is reported for the scaled critical trace parameters. Scaling performance reported by Xiao et al. (2020) exceeds the scaling results obtained using ARTIST for the dataset under investigation.

The work of Xue et al. (2022) is, to our best knowledge, the only work that applies deep learning to all three ionogram types. In their investigation, separate convolutional models were used to perform ionogram classification (VIS, OIS or BSS) and trace segmentation. The results reported by Xue et al. (2022) are only provided for the classification model and hence a comparative performance assessment of feature extraction cannot be undertaken.

To the best of our knowledge, no investigations have been conducted for the application of Transformer-based models for ionogram scaling application. Visual Transformer (ViT) models have surpassed the performance of convolutional models for image classification²⁰ and therefore should be reviewed for ionogram scaling applications, particularly for the OIS and BSS categories for which limited scaling solutions are available. This represents an opportunity for further research.

XI. DISCUSSION

This section includes a discussion of insights, findings and recommendations based on the literature review conducted for ionogram scaling. This material can be used to guide and stimulate further research in this field.

Finding 1: Lack of an ionogram benchmark dataset

²⁰See <https://www.paperswithcode.com/sota/image-classification-on-imagenet> for a leaderboard snapshot of image classification models evaluated against the ImageNet benchmark dataset.

Variability Feature	Time Scale	Spatial Scale	Comments
Diurnal	24hr	global	Higher levels of ionisation occur during the day versus night. The E and F1 layers disappear at night leaving only a weakened F2 layer. Consequently, night time ionograms do not have traces corresponding to the E and F1 layers. See Davies (1990).
Sunrise and sunset	minutes	global	Passage of the dawn and dusk terminators result in highly dynamic transformations of the ionosphere (Cervera et al., 2021). This imposes strong Doppler shifts on the radio wave signal which will be apparent on sounders which measure Doppler such as the Digisonde.
Seasonal	1-3 months	global	The level of ionisation varies significantly with season. The E and F1 layers are strongest in summer and weakest in winter. However, during the day, and especially in the northern hemisphere, F2 layer is stronger in winter than in summer (the winter anomaly) (Davies, 1990). This is due to slower ion loss processes in the winter F2 layer.
Solar cycle	11 years	global	Solar activity varies periodically in cycles of approximately 11 years. In general, higher frequency values for ionospheric layer trace returns are observed near the peak of the solar cycle (Davies, 1990).
Latitudinal	N/A	thousands km	The strength of the ionosphere varies significantly with latitude. The strength of the E and F1 layers peaks at the sub-solar latitude near the equator whereas the F2 layer strength peaks at approximately 15 degrees north and south of the geomagnetic equator known as the Appleton Anomaly regions (Davies, 1990).

TABLE V: Summary of influence of solar variability on ionogram feature characteristics.

Irregularity Feature	Time Scale	Spatial Scale	Comments
Sporadic E (Es)	hours	tens - hundreds km	The sporadic E layer, Es, is a thin layer of concentrated metallic ions. Additional traces and features will be evident in VIS, OIS and BSS ionograms. In some cases the Es layer can obscure the F layer returns in VIS ionograms, especially at lower frequencies.
Meteor	seconds	small	Reflections from transient meteors manifest on an ionogram at low group ranges. These returns are easily identifiable and able to be separated from main ionospheric layer returns. However in some cases they can contribute to ionogram feature and propagation mode classification issues (Heitmann and Gardiner-Garden, 2019).
Solar flare	minutes-hours	large	Intense, short-term bursts of X-rays originating from solar flares significantly increase the strength of the D layer of the ionosphere resulting in enhanced absorption of HF radio waves. Consequently, a portion of, or in some extreme cases, the complete HF band can be “blocked” out for HF propagation. Aspects of, or entire ionospheric layer returns can be masked out on an ionogram recording.
Ionospheric irregularities	N/A	thousands km	Ionospheric electrodynamics vary as a function of geomagnetic location (equatorial, mid-latitude, auroral/polar). Ionospheric irregularities may occur in each of these regions and are due to different electrodynamic processes. The irregularities can cause range and/or frequency spreading of the signal. When the F layer returns are affected, this is referred to as spread F.
Small Scale TID (SSTID)	minutes	tens km	Small Scale Traveling Ionospheric Disturbances (SSTIDs) may have a large effect on ionospheric soundings with very complicated multiple oscillatory and “splitting” features in the ionogram traces being evident (Cervera et al., 2021). Very small scale SSTIDs (~25km) may cause spread F (Cervera et al., 2021).
Medium Scale TID (MSTID)	minutes	hundreds km	MSTIDs may be generated by atmospheric gravity waves in the neutral atmosphere perturbing the ionospheric plasma or by electrodynamic processes within the ionosphere. They cause additional cusp or “loop” features in VIS ionograms (Cervera and Harris, 2014), complex curve features (or “kinks”) in OIS ionograms (Heitmann et al., 2018) and introduce additional leading edges in BSS ionograms (Croft, 1972).
Large Scale TID (LSTID)	hours	thousands km	LSTIDs, generated primarily in the auroral regions, cause the ionosphere to vary slowly. The effect of LSTIDs is not noticeable at the resolution of a single VIS ionogram. Analysis of a series of VIS ionograms is required to confirm a pattern of virtual height and critical frequency variations due to LSTIDs (Pederick et al., 2017). Consequently LSTIDs do not pose a problem for the scaling of VIS ionograms. However, strong LSTIDs may cause additional oblique propagation paths which manifest as additional “satellite” traces on OIS ionograms (Heitmann, 2018) and pose a challenge for automated scaling algorithms.
Chordal Modes	N/A	N/A	Steep gradients in the equatorial ionosphere can affect propagation path characteristics for north-south oriented paths. In these cases, the sounder transmission signals may not follow a “direct” path from the transmitter to the receiver (OIS) or ground (BSS) via the ionosphere, but rather follow a more complicated path where the radio waves “skip” across the geomagnetic equator between the north and south equatorial Appleton Anomaly regions (Cervera et al., 2021). This phenomenon enables propagation over long distances. Chordal propagation modes manifest on BSS ionograms as isolated, strong echoes at long group ranges.

TABLE VI: Summary of the effects of natural phenomena on ionogram characteristics.

The success of deep learning is largely attributed to the availability of publically available benchmark datasets. For example, the Cityscapes dataset (Cordts et al., 2016) is a large collection of images relating urban street scenes that includes pixel-level annotations. This dataset is commonly used to measure, report and compare deep learning segmentation model performance. Our review has found that an equivalent benchmark dataset does not exist for ionogram scaling. Fair and transparent comparative evaluation of automatic

ionogram scaling techniques and algorithms is difficult to perform due to a lack of a benchmark dataset. Ionogram scaling publications reference custom datasets that vary in data size and diversity, and are seldom publically available.

Recommendation 1: Development of an ionogram scaling benchmark dataset

An authoritative ionograms scaling benchmark dataset

should be developed. This dataset should encompass all three sounder types to address the unique ionogram characteristics pertaining to each. Resources such as Reinisch and Galkin (2011) can be leveraged to accelerate this effort.

Some factors to be considered in the design of an ionogram scaling benchmark dataset include:

- *Manual scaling of labels should be authored by a group of Subject Matter Experts with a diverse ionogram scaling experience.*

Ionogram scaling labels need to account for the subjective interpretation nature of the ionogram feature set, and hence a diverse composition of scaling experience is encouraged for the benchmark dataset. This is particularly important for labeling of ionograms displaying the effects of ionospheric disturbances, and ionograms recorded by a BSS sounder in general.

- *Include labels generated by authoritative scaling tools.*
Inclusion of labels generated by authoritative scaling tools (where such tools are available, e.g. ARTIST for VIS ionograms), will enable a transparent, repeatable comparative scaling performance evaluation of scaling techniques.

- *Strive for a diverse and balanced dataset design.*

The variability of the ionosphere is well known, and studies such as (Hunsucker, 1970) (Croft, 1972) (Penzin et al., 2019) show that less 10% of ionograms can be described as originating from ‘quiet’ ionospheric conditions. Consequently, a benchmark dataset should be comprised of a balanced and diverse composition of ionograms. Space weather variability and irregularity factors as described in Tables V and VI can be used to guide the design of a benchmark dataset.

The dataset should also include meta-data that describes the inferred ionosphere conditions and sounder configuration parameters referenced for each ionogram. This information is valuable for informed scaling model performance assessment, including model generalisation. See Galkin et al. (1999) for analysis of meta data requirements for an internet ionospheric data repository. In addition, this information can also be used to enable implementation of class weighting approaches (Gong et al., 2019) during model development to compensate for unbalanced datasets. The convention adopted by ARTIST (Galkin et al., 2013) for the evaluation and reporting of ionogram data quality for VIS ionograms can be used as an exemplar, and be expanded to cover OIS and BSS ionogram datasets.

Finding 2: Lack of a scaling standard for the BSS ionogram

The URSI scaling standard (Piggott and Rawer, 1978) defines metrics for the evaluation of VIS ionogram scaling performance. The metrics are defined in terms of acceptability and accuracy referenced to frequency and group range dimensions (discussed earlier in Section V) and is very useful for gauging and comparing automatic scaling performance. The

vast majority of VIS scaling investigations use these metrics for reporting scaling performance.

Whilst no official scaling standard is defined for OIS ionograms, the VIS scaling standard (Piggott and Rawer, 1978) is commonly referenced in OIS scaling investigations. This practice is deemed acceptable due to the similarity of OIS and VIS trace feature characteristics. No equivalent scaling standard exists for the evaluation of BSS ionogram scaling performance. Without such a standard, existing BSS scaling investigations report performance using custom metrics.

Recommendation 2: Define and standardise metrics for the evaluation of BSS ionogram scaling

The LE features of a BSS ionogram do not resemble the features embedded in VIS and OIS ionograms, hence a dedicated scaling standard is required. An obvious metric is based on the pixel-wise distance between the estimated and truth (manually labelled) LE traces for each ionospheric layer return. This distance can be reported in frequency and/or group range dimensions. Given that a BSS ionogram LE trace exhibits an undefined length with no fixed start or end coordinates, a decision needs to be made on how many, and which LE pixels should be used as reference pixels for metric calculations.

One approach to resolve this dilemma is to divide the LE trace into a fixed number of equally spaced segments, and use the pixel coordinates of each segment for evaluation purposes. One disadvantage of this technique is that the coordinates of each reference pixel will vary from one ionogram to another due to the differences in the LE trace profile (trace length, and start and end coordinates). This will render the evaluation mechanism unrepeatable across datasets. An alternative approach is to select a fixed number of evaluation coordinates, defined in group-range or frequency dimensions, and use these coordinates as reference points for evaluation purposes. This approach is used by Song et al. (2015) and Crouch (2018), where 5 pre-defined, identical frequency and group-range values respectively are used to evaluate the distance of estimated LE trace to truth across the full dataset. Figure 9 depicts this metric approach for a sample BSS ionogram. The benefit of this approach is that the reference LE pixels are identical across the ionograms, and this enables a repeatable and transparent evaluation. A potential problem with this proposed technique is that it is not guaranteed that a LE trace will coincide with all group-range reference values (i.e. the LE trace may not extend across the span of group-range represented by the reference values). In this situation, the associated reference group-range value can be omitted during metric calculations.

It is recommended that the URSI scaling standard (Piggott and Rawer, 1978) for reporting scaling performance in terms of ratio of results that are deemed as accurate and acceptable (based on error margins as discussed earlier in Section V) is also adopted for reporting BSS scaling performance. In addition to including metrics that report scaling performance in terms of accuracy, metrics that account for recall rate i.e.

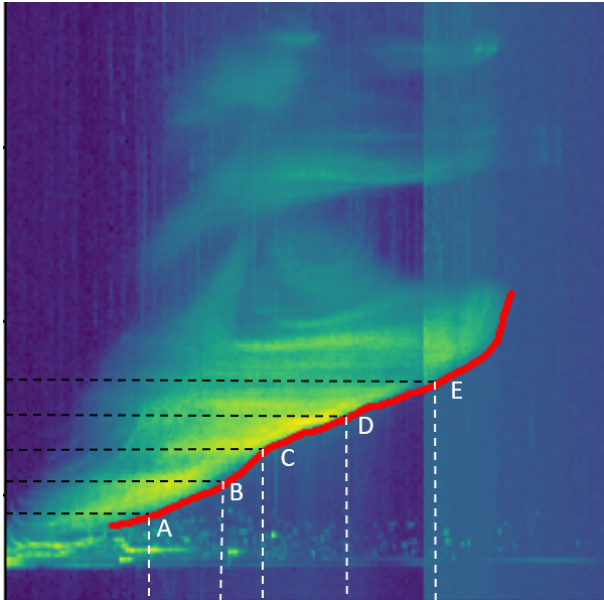


Fig. 9: This diagram displays one approach that can be adopted for standardising BSS scaling performance evaluation. A set of 5 group-range lines (dashed black lines) is used to derive 5 unique LE reference pixel coordinates (labelled as A-E) that can be used to quantify the frequency scaling error (dashed white lines) obtained from a LE extraction model.

ratio of LE pixels that were not found by the LE extraction model (False Negatives), should also be considered.

Recommendation 3: Conduct an experimental study to evaluate, compare and demonstrate the effectiveness of scaling methods and techniques

An experimental based, case-study comparing ionogram scaling solutions generated by a suite of scaling tools and methods would be extremely useful to the ionospheric research community. Some reviews of this nature have been performed for a pairwise assessment of VIS scaling tools e.g. ARTIST vs Autoscala (Pezzopane and Scotto, 2005, 2007), however to the best of our knowledge, no comparative experimental studies have been performed across all sounder types. This study should evaluate scaling tools and methods in multiple geographical locations and ionospheric conditions.

Recommendation 4: Continue research of deep learning techniques for automatic ionogram scaling

Transformation of image semantics contextualised by human experience in a scientific domain into a set of instructions that can be coded with a programming language is extremely challenging. The subjective interpretation aspect and requirement to codify all possible edge cases and domain specific nuances renders the task of automated software solutions that produce accurate and repeatable outcomes at scale without human intervention almost impossible to achieve. The recent

advent of deep learning can address some aspects of this challenge.

Deep learning has made noteworthy advancements over the last decade to achieve a high level of success in computer vision tasks such as image recognition, object detection and image segmentation. Segmentation, a pixel-level classification of an image into semantic regions of interest, is of particular relevance to ionogram scaling. Convolutional (Minaee et al., 2021), and recently, transformer based methods (Li et al., 2023), are utilised to develop state-of-the-art image segmentation models that are producing remarkable performance against open-source benchmark image datasets.

Ionogram scaling can benefit from the ability of deep learning segmentation models to learn salient, spatial relationships at local and global scales related to pixel intensity, edges, contours and shapes in an ionogram image. This capability can be particularly useful for scaling of ionograms that are captured in disturbed ionospheric conditions where image features can be occluded, distorted or separated. Moreover, the challenge of identification of LE features in a BSS ionogram may not be adequately satisfied through the use of conventional techniques that have been successful for VIS and OIS ionograms. For this case, the adoption of deep learning segmentation methodologies may be the most beneficial.

Opportunities for research on deep learning segmentation models for automatic ionogram scaling application, includes, but is not limited to the following:

- Application of Vision Transformer models for ionogram feature extraction. Transformer model design has demonstrated a performance edge over convolutional based models in the computer vision domain.
- Use of semi-supervised, self-supervised segmentation model designs, transfer learning and/or custom data augmentation techniques. These approaches can alleviate the dataset labelling burden.
- Integration of radio wave propagation theory and ionospheric physics with deep learning to produce a physics guided deep learning ionogram scaling model.

It is anticipated that the release of annotated ionogram scaling datasets will accelerate the research of deep learning for application to ionogram scaling. Data science competitions, such as Kaggle (Banachewicz et al., 2022), have stimulated deep learning research for diverse applications, through the use of large, open-source datasets.

XII. CONCLUSION

The ionosphere is a highly dynamic medium, hence characterisation of the ionosphere is crucial for the effective operation of any HF system. Vertical, oblique and backscatter sounders are used to record bottomside measurements of the ionosphere to enable quantification of its properties. The task of analysing, identifying and extracting features from ionospheric measurements (ionograms), known as scaling, is a time intensive and laborious process and so a number of automated scaling techniques and tools have been developed over the last few decades. The proliferation of vertical sounder networks globally has stimulated research and development of

scaling algorithms for the vertical sounder, and hence it is not surprising that the majority of publications focus on the vertical sounder application.

In this paper, we have reviewed the techniques for automated scaling across all ground-based ionospheric sounder systems. To the best of our knowledge, this is the first comparative review across all sounder types. A review of ionogram features, toolsets and metrics for each sounder is presented. In addition, an analysis of the impact of ionospheric irregularities and disturbances on the ionogram scaling challenge is also included.

Furthermore, we have included a discussion of our findings and recommendations that we hope will accelerate reproducible research in this field to expedite progress for automated scaling of ionograms recorded by all types of sounder systems. We believe that the development of an ionogram scaling benchmark dataset and metric standardisation will stimulate further research in this field and draw participation of the deep learning community. This can be particularly beneficial for the oblique and backscatter sounder systems for which there is a limited number of automated scaling solutions available.

An automated scaling ionogram capability enables real-time characterisation and forecasting of ionospheric properties derived from large global ionospheric datasets recorded by vertical, oblique and backscatter sounder systems. This is a crucial requirement for supporting of HF systems that exploit the ionosphere to provide a beyond line-of sight capability such as communications, surveillance, navigation or remote sensing.

ACKNOWLEDGMENTS

We thank Lenard Pederick, Andrew Heitmann and David Holdsworth for useful discussions, reviews and suggestions related to writing this paper.

We thank Lenard Pederick and Andrew Heitmann for generating Figures 3 and 6 respectively.

REFERENCES

- Arikan, F., O. Arikan, and S. Salous (2002). A new algorithm for high-quality ionogram generation and analysis. *Radio Science* 37(1), 1–11.
- Australian Space Weather Forecasting Centre (2022). Scaled Ionospheric Data Format. Retrieved from https://www.sws.bom.gov.au/World_Data_Centre/1/3.
- Ayliffe, J. K., L. J. Durbridge, G. J. Frazer, R. S. Gardiner-Garden, A. J. Heitmann, J. Praschifka, A. D. Quinn, G. C. Scarman, and M. D. E. Turley (2019). The DST Group High-Fidelity, Multichannel Oblique Incidence Ionosonde. *Radio Science* 54(1), 104–114.
- Banachewicz, K., L. Massaron, and A. Goldbloom (2022). *The Kaggle Book: Data analysis and machine learning for competitive data science*. Packt Publishing.
- Becker, W. (1967). On the manual and digital computer methods used at lindau for the conversion of multifrequency ionograms to electron density-height profiles. *Radio Science* 2(10), 1205–1232.
- Bland, E. C., A. J. McDonald, S. de Larquier, and J. C. Devlin (2014). Determination of ionospheric parameters in real time using SuperDARN HF Radars. *Journal of Geophysical Research: Space Physics* 119(7), 5830–5846.
- Cervera, M. A. and T. J. Harris (2014). Modeling ionospheric disturbance features in quasi-vertically incident ionograms using 3-d magnetoionic ray tracing and atmospheric gravity waves. *Journal of Geophysical Research: Space Physics* 119(1), 431–440.
- Cervera, M. A., T. J. Harris, D. A. Holdsworth, and D. J. Netherway (2021). *Ionospheric Effects on HF Radio Wave Propagation*, pp. 439–492. Geophysical Monograph Series.
- Chen, G., Z. Zhao, S. Li, and S. Shi (2009). Wiobss: The chinese low-power digital ionosonde for ionospheric backscattering detection. *Advances in Space Research* 43(9), 1343–1348.
- Chen, Z., Z. Gong, F. Zhang, and G. Fang (2018). A New Ionogram Automatic Scaling Method. *Radio Science* 53(9), 1149–1164.
- Chen, Z., S. Wang, S. Zhang, G. Fang, and J. Wang (2013). Automatic scaling of F layer from ionograms. *Radio Science* 48(3), 334–343.
- Conkright, R. O. and L. F. McNamara (1997). Quality control of automatically scaled vertical incidence ionogram data. *Radio Science* 32(5), 1997–2002.
- Cordts, M., M. Omran, S. Ramos, T. Rehfeld, M. Enzweiler, R. Benenson, U. Franke, S. Roth, and B. Schiele (2016). The Cityscapes Dataset for Semantic Urban Scene Understanding. In *2016 IEEE Conference on Computer Vision and Pattern Recognition (CVPR)*, pp. 3213–3223.
- Croft, T. A. (1972). Sky-wave backscatter: A means for observing our environment at great distances. *Reviews of Geophysics* 10(1), 73–155.
- Crouch, C. (2018). *Using neural networks and deep learning to improve ionospheric model accuracy using high-frequency radar backscatter observations*. Masters Research Thesis, University of Adelaide.
- Davies, K. (1990). Books. doi:10.1049/PBEW031E.
- De La Jara, C. and C. Olivares (2021). Ionospheric Echo Detection in Digital Ionograms Using Convolutional Neural Networks. *Radio Science* 56(8), e2020RS007258. e2020RS007258 2020RS007258.
- Ding, Z., B. Ning, W. Wan, and L. Liu (2007). Automatic scaling of F2-layer parameters from ionograms based on the empirical orthogonal function (EOF) analysis of ionospheric electron density. *Earth, Planets and Space* 59(1), 51–58.
- Doupnik, J. R. and E. R. Schmerling (1965). The reduction of ionograms from the bottomside and topside. *Journal of Atmospheric and Terrestrial Physics* 27(8), 917–941.
- Dyson, P., J. Devlin, R. Norman, and M. Parkinson (2000). The TIGER radar: An extension of SuperDARN to subauroral latitudes. *Workshop on Applications of Radio Science Proceedings*, 9–31.
- Dyson, P. L. and J. A. Bennett (1988). A model of the vertical distribution of the electron concentration in the ionosphere and its application to oblique propagation studies. *Journal of Atmospheric and Terrestrial Physics* 50(3), 251–262.
- Earl, G. F. and B. D. Ward (1987). The frequency management

- system of the Jindalee over-the-horizon backscatter HF radar. *Radio Science* 22(2), 275–291.
- Fagre, M., J. A. Prados, J. Scandaliaris, B. S. Zossi, M. A. Cabrera, R. G. Ezquer, and A. G. Elias (2021). Algorithm for Automatic Scaling of the F-Layer Using Image Processing of Ionograms. *IEEE Transactions on Geoscience and Remote Sensing* 59(1), 220–227.
- Fox, M. W. and C. Blundell (1989). Automatic scaling of digital ionograms. *Radio Science* 24(6), 747–761.
- Galkin, A., B. Reinisch, X. Huang, and G. Khmyrov (2013). Confidence Score of ARTIST-5 Ionogram Autoscaling. https://www.ursi.org/files/CommissionWebsites/INAG/web-73/confidence_score.pdf. Accessed on 02 December, 2024.
- Galkin, I. and B. Reinisch (2008). The new artist 5 for all digisondes. *Ionosonde Network Advisory Group* 69.
- Galkin, I. A., D. F. Kitrosser, Z. Kecic, and B. W. Reinisch (1999). Internet access to ionosondes. *Journal of Atmospheric and Solar-Terrestrial Physics* 61(1), 181–186.
- Galkin, I. A., B. W. Reinisch, X. Huang, and D. Bilitza (2012). Assimilation of GIRO data into a real-time IRI. *Radio Science* 47(04), 1–10.
- Galkin, I. A., B. W. Reinisch, G. A. Ososkov, E. G. Zaznobina, and S. P. Neshyba (1996). Feedback neural networks for ARTIST ionogram processing. *Radio Science* 31(5), 1119–1128.
- Gardiner-Garden, R., A. Heitmann, and N. Brett (2018). A Parametric Model of the Ionosphere Electron Density Profile for JORN. DST-Group-TN-1722.
- Gladden, S. C., L. Central Radio Propagation, L. Boulder, and S. United (1959). *A history of vertical-incidence ionosphere sounding at the National Bureau of Standards*. National Bureau of Standards technical note ;28. Washington, D. C.: U.S. Dept. of Commerce, National Bureau of Standards : U.S. Govt. Print. Off.
- Gong, Z., P. Zhong, and W. Hu (2019). Diversity in Machine Learning. *IEEE Access* 7, 64323–64350.
- Haldoupis, C., D. Pancheva, W. Singer, C. Meek, and J. Macdougall (2007). An explanation for the seasonal dependence of midlatitude sporadic e layers. *J. Geophys. Res.* 112.
- Harris, T. J., A. D. Quinn, and L. H. Pederick (2016). The DST group ionospheric sounder replacement for JORN. *Radio Science* 51(6), 563–572.
- Heitmann, A. J., M. A. Cervera, R. S. Gardiner-Garden, D. A. Holdsworth, A. D. MacKinnon, I. M. Reid, and B. D. Ward (2018). Observations and modeling of traveling ionospheric disturbance signatures from an australian network of oblique angle-of-arrival sounders. *Radio Science* 53(9), 1089–1107.
- Heitmann, A. J. and R. S. Gardiner-Garden (2019). A Robust Feature Extraction and Parameterized Fitting Algorithm for Bottom-Side Oblique and Vertical Incidence Ionograms. *Radio Science* 54(1), 115–134.
- <https://github.com/space-physics/POLAN> (2017). Polan. Retrieved from <https://github.com/space-physics/POLAN>.
- Hu, Y., H. Song, X. Zou, and Z. Zhao (2015). Real-time automatic scaling method of oblique ionogram parameters based on morphological operator and inversion technique. *Wuhan University Journal of Natural Sciences* 20(4), 323–328.
- Hunsucker, R. D. (1970). *An atlas of oblique-incidence high-frequency backscatter ionograms of the midlatitude ionosphere*. ESSA technical report ERL ; 162. ITS ; 104. Boulder, Colorado: U.S. Department of Commerce, Environmental Science Services Administration, Research Laboratories, Institute for Telecommunication Sciences. Includes bibliographical references (pages 105–108).
- Hunsucker, R. D. (1991). Radio techniques for probing the terrestrial ionosphere. *Physics and Chemistry in Space* 22.
- Hutchinson, S. T. (1994). Scaling backscatter 1F leading edges. Internal Report, DST Group.
- Igi, Nozaki, Nagayama, Ohtani, Kato, and Igarashi (1993). Automatic ionogram processing systems in Japan. <https://www.ursi.org/files/CommissionWebsites/INAG/uag-104/ext/igi.html>. Accessed on 31 January, 2025.
- Ippolito, A., C. Scotto, D. Sabbagh, V. Sgrigna, and P. Maher (2016). A procedure for the reliability improvement of the oblique ionograms automatic scaling algorithm. *Radio Science* 51(5), 454–460.
- Jiang, C., G. Yang, T. Lan, P. Zhu, H. Song, C. Zhou, X. Cui, Z. Zhao, and Y. Zhang (2015). Improvement of automatic scaling of vertical incidence ionograms by simulated annealing. *Journal of Atmospheric and Solar-Terrestrial Physics* 133, 178–184.
- Jiang, C., G. Yang, Z. Zhao, Y. Zhang, P. Zhu, and H. Sun (2013). An automatic scaling technique for obtaining F2 parameters and F1 critical frequency from vertical incidence ionograms. *Radio Science* 48(6), 739–751.
- Jiang, C., G. Yang, Y. Zhou, P. Zhu, T. Lan, Z. Zhao, and Y. Zhang (2016). Software for scaling and analysis of vertical incidence ionograms-ionoscaler. *Advances in Space Research* 59.
- LeCun, Y., Y. Bengio, and G. Hinton (2015). Deep learning. *Nature* 521(7553), 436–444.
- Li, X., H. Ding, H. Yuan, W. Zhang, J. Pang, G. Cheng, K. Chen, Z. Liu, and C. C. Loy (2023). Transformer-based visual segmentation: A survey. *arXiv preprint arXiv:2304.09854*.
- Lynn, K. J. W. (2018). Histogram-based ionogram displays and their application to autoscaling. *Advances in Space Research* 61(5), 1220–1229.
- Maruyama, T., M. Kawamura, S. Saito, K. Nozaki, H. Kato, N. Hemmakorn, T. Boonchuk, T. Komolmis, and C. Ha Duyen (2007). Low latitude ionosphere-thermosphere dynamics studies with inosonde chain in Southeast Asia. *Ann. Geophys.* 25(7), 1569–1577. ANGEO.
- McDonnell, M. (2014). Wavelet based detection and fitting of backscatter ionogram leading edges.
- McNamara, L. F. (2006). Quality figures and error bars for autoscaled Digisonde vertical incidence ionograms. *Radio Science* 41(4).
- Minaee, S., Y. Boykov, F. Porikli, A. Plaza, N. Kehtarnavaz, and D. Terzopoulos (2021). Image Segmentation Using Deep Learning: A Survey. *IEEE transactions on pattern analysis and machine intelligence* PP.
- Mochalov, V. and A. Mochalova (2019). Extraction of ionosphere parameters in ionograms using deep learning. *E3S Web of Conferences* 127, 01004.

- Netherway, D. J., M. J. Whitington, and R. S. Gardiner-Garden (2018). High Range Resolution Backscatter Sounder Ionograms. *DST-Group-TR-3477*.
- Nickisch, L. J., S. Fridman, M. Hausman, and G. S. San Antonio (2016). Feasibility study for reconstructing the spatial-temporal structure of TIDs from high-resolution backscatter ionograms. *Radio Science* 51(5), 443–453.
- Pederick, L. H., M. A. Cervera, and T. J. Harris (2017). Interpreting observations of large-scale traveling ionospheric disturbances by ionospheric sounders. *Journal of Geophysical Research: Space Physics* 122(12), 12,556–12,569.
- Penzin, M. S., S. N. Ponomarchuk, V. P. Grozov, and V. I. Kurkin (2019). Real-Time Techniques for Interpretation of Ionospheric Backscatter Sounding Data. *Radio Science* 54(5), 480–491.
- Pezzopane, M. (2004). Software for the automatic scaling of critical frequency f0F2 and MUF(3000)F2 from ionograms applied at the Ionospheric Observatory of Gibilmanna. *Annals of Geophysics* 47(6).
- Pezzopane, M. and C. Scotto (2005). The ingy software for the automatic scaling of fof2 and muf(3000)f2 from ionograms: A performance comparison with artist 4.01 from rome data. *Journal of Atmospheric and Solar-Terrestrial Physics*, 1063–1073.
- Pezzopane, M. and C. Scotto (2007). Automatic scaling of critical frequency foF2 and MUF (3000) F2: A comparison between Autoscala and ARTIST 4.5 on Rome data. *Radio Science* 42.
- Pezzopane, M. and C. Scotto (2008). A method for automatic scaling of F1 critical frequencies from ionograms. *Radio Science* 43(2).
- Pezzopane, M. and C. Scotto (2010). Highlighting the F2 trace on an ionogram to improve Autoscala performance. *Computers and Geosciences* 36(9), 1168–1177.
- Pezzopane, M., C. Scotto, L. Tomasik, and I. Krasheninnikov (2010). Autoscala: an aid for different ionosondes. *Acta Geophysica* 58(3), 513–526.
- Piggott, W. R. and K. Rawer (1978). U.R.S.I. handbook of ionogram interpretation and reduction. (Karl).
- Pillat, V., L. Guimarães, P. Fagundes, and J. Silva (2013). A computational tool for ionosonde CADI's ionogram analysis. *Computers and Geosciences* 52, 372–378.
- Redding, N. J. (1996). Image understanding of oblique ionograms: the autoscaling problem. In *1996 Australian New Zealand Conference on Intelligent Information Systems. Proceedings. ANZIIS 96*, pp. 155–160.
- Reinisch, B. W. and I. A. Galkin (2011). Global Ionospheric Radio Observatory (GIRO). *Earth, Planets and Space* 63(4), 377–381.
- Reinisch, B. W., I. A. Galkin, G. M. Khmyrov, A. V. Kozlov, K. Bibl, I. A. Lisysyan, G. P. Cheney, X. Huang, D. F. Kitrosser, V. V. Paznukhov, Y. Luo, W. Jones, S. Stelmash, R. Hamel, and J. Grochmal (2009). New Digisonde for research and monitoring applications. *Radio Science* 44(1).
- Reinisch, B. W., R. R. Gamache, H. Xueqin, and L. F. McNamara (1988). Real time electron density profiles from ionograms. *Advances in Space Research* 8(4), 63–72.
- Reinisch, B. W., X. Huang, I. A. Galkin, V. Paznukhov, and A. Kozlov (2005). Recent advances in real-time analysis of ionograms and ionospheric drift measurements with digisondes. *Journal of Atmospheric and Solar-Terrestrial Physics* 67(12), 1054–1062.
- Reinisch, B. W. and H. Xueqin (1983). Automatic calculation of electron density profiles from digital ionograms: 3. Processing of bottomside ionograms. *Radio Science* 18(3), 477–492.
- Scotto, C. (2001). A method for processing ionograms based on correlation technique. *Physics and Chemistry of the Earth, Part C: Solar, Terrestrial and Planetary Science* 26(5), 367–371.
- Scotto, C. and M. Pezzopane (2007). A method for automatic scaling of sporadic e layers from ionograms. *Radio Science* 42(2).
- Song, H., Y. Hu, C. Jiang, C. Zhou, and Z. Zhao (2015). Automatic scaling of HF swept-frequency backscatter ionograms. *Radio Science* 50(5), 381–392.
- Song, H., Y. Hu, C. Jiang, C. Zhou, Z. Zhao, and X. Zou (2016). An automatic scaling method for obtaining the trace and parameters from oblique ionogram based on hybrid genetic algorithm. *Radio Science* 51(12), 1838–1854.
- Su, F., Z. Zhao, S. Li, M. Yao, G. Chen, and Y. Zhou (2012). Signal Identification and Trace Extraction for the Vertical Ionogram. *IEEE Geoscience and Remote Sensing Letters* 9(6), 1031–1035.
- Theera-Umpon, N. (2007). *Ionospheric F-Layer Critical Frequency Estimation from Digital Ionogram Analysis*, Volume 4707.
- Themens, D., B. Reid, and S. Elvidge (2022). ARTIST ionogram autoscaling confidence scores: best practices. *URSI Radio Science Letters* 4, 1–5.
- Titheridge, J. E. (1961). A new method for the analysis of ionospheric h'(f) records. *Journal of Atmospheric and Terrestrial Physics* 21(1), 1–12.
- Titheridge, J. E. (1967). The Overlapping-Polynomial Analysis of Ionograms. *Radio Science* 2(10), 1169–1175.
- Titheridge, J. E. (1969). Single-Polynomial Analysis of Ionograms. *Radio Science* 4(1), 41–51.
- Titheridge, J. E. (1975). The relative accuracy of ionogram analysis techniques. *Radio Science* 10(6), 589–599.
- Titheridge, J. E. (1985). Ionogram analysis with the generalised program POLAN.
- Titheridge, J. E. (1988). Real height analysis of ionograms - a generalized formulation. 23.
- Tsai, L.-C. and F. T. Berkey (2000). Ionogram analysis using fuzzy segmentation and connectedness techniques. *Radio Science* 35(5), 1173–1186.
- Whitehead, J. D. (1989). Recent work on mid-latitude and equatorial sporadic-E. *Journal of Atmospheric and Terrestrial Physics* 51(5), 401–424.
- Wright, J. (1959). *Mean electron density variations of the quiet ionosphere*. US Department of Commerce, Office of Technical Services.
- Wright, J. and L. A. Fine (1960). Mean Electron Density Variations of the Quiet Ionosphere 2 - April 1959. *NATIONAL BUREAU OF STANDARDS*.
- Xiao, Z., J. Wang, J. Li, B. Zhao, L. Hu, and L. Liu (2020).

Deep-learning for ionogram automatic scaling. *Advances in Space Research* 66(4), 942–950.

Xue, J., C. Zhang, B. Yin, X. Jia, J. Xu, and M. Ma (2022). Ionogram Echo Extraction Based on the Convolutional Neural Networks. *Radio Science* 57(6), e2022RS007459. e2022RS007459 2022RS007459.

Zheng, Wang, Luo, Tian, and Chen (2022, Aug ,). Segmentation and Edge Detection for Ionogram Automatic Scaling.